Inhibition of the initial stages of corrosion by 2-mercaptobenzothiazole adsorption and the effects of interfacial oxides on copper in neutral chloride conditions

Vishant Garg, Sandrine Zanna, Antoine Seyeux, Frédéric Wiame, Vincent Maurice, Philippe Marcus

Author preprint published in Corrosion Science
https://doi.org/10.1016/j.corsci.2023.111596

Inhibition of the initial stages of corrosion by 2-mercaptobenzothiazole adsorption and the effects of interfacial oxides on copper in neutral chloride conditions

Vishant Garg, Sandrine Zanna, Antoine Seyeux,

Frédéric Wiame, Vincent Maurice[1], Philippe Marcus[2]

PSL University, CNRS – Chimie ParisTech, Institut de Recherche de Chimie Paris,

Physical Chemistry of Surfaces Research Group,

11 rue Pierre et Marie Curie, 75005 Paris, France.

Abstract

Advanced surface analytical techniques were used to study 2-mercaptobenzothiazole (2-MBT) adsorption and interfacial oxide effects on copper, and cyclic voltammetry was used to characterize corrosion inhibition in NaCl solution. 2-MBT adsorbs on metallic copper by its sulphur atoms along with a small fraction of nitrogen atoms. The 2-MBT film formed is thicker when the interfacial oxide is less. Upon anodic polarisation, a direct correlation between the thickness of 2-MBT layer and protection against corrosion initiation is observed. The metal-organic complexes, formed by an interaction between 2-MBT and Cu(I) ions, do not offer additional protection to the substrate.

Keywords

A – Copper; A – Organic Inhibitor; A – 2-mercaptobenzothiazole; B – Cyclic Voltammetry; B – XPS; B – ToF-SIMS; C – Corrosion Inhibition.

[1] Corresponding author: vincent.maurice@chimieparistech.psl.eu
[2] Corresponding author: philippe.marcus@chimieparistech.psl.eu

Introduction

The aqueous corrosion of copper has been studied extensively due to the wide use of the metal and its alloys, and the degradation that can result from exposure to the natural elements. One environmental species that has major consequences on the corrosion behaviour of copper and other metals is chloride ions. On copper, chloride ions compete with water molecules for adsorption on the metal surface and thus poison or even block the formation of the passive oxide film that otherwise provides protection to the substrate in pH conditions where copper oxides are stable (pH > 5) [1–3]. On passivated copper surfaces, chloride ions can adsorb and penetrate the surface oxide film, causing passivity breakdown followed by initiation of localised corrosion (pitting) with the formation of copper chlorides [4–7]. The breakdown of the passive oxide film has been widely discussed and it has been proposed to occur locally at weak sites of the protective layer including grain boundaries and defective sites in the oxide film [1,8–11]. Other factors influencing the corrosion mechanism such as chloride concentration, temperature, pH of the environment, and even the structure of the oxide films on the copper surface have been investigated [7,8,12–15].

2-mercaptobenzothiazole (2-MBT) is an organic inhibitor that can protect copper from corrosion in varying degrees depending on the environment and its pH, the surface state of the metal substrate, and the concentration of the inhibitor [16–28]. It is used due to its dexterity as a mixed-type inhibitor, restricting both anodic and cathodic reactions that may occur on the metal surface [29,30]. Several works have discussed the adsorption of 2-MBT on metallic surfaces and on oxidized surfaces from vapour phase [16–18] and from various aqueous solutions [19–27,31]. It is reported that the bonding between the molecule and metallic copper mostly involves the sulphur atoms of the molecule due to the affinity of sulphur to copper [16,20–22]. However, some studies have revealed that a fraction of the adsorbed molecules also bond to the metallic substrate via the nitrogen atom [17,19]. The interaction between the 2-MBT molecule and the copper oxides is not fully understood. Density functional theory (DFT) modelling has shown that dense organic monolayers can form on Cu(I) oxide-covered surfaces. It also suggests that besides covalent bonding between the S atoms of the molecules and Cu(I) ions of the covering oxide, there can be a hydrogen bonding between the NH group of the molecule and the surface oxygen atoms (for the thione conformer), or between the N atom and the Cu(I) ions (for the thiolate conformer) [21,32,33].

However, the possibility of N(H) bonding has eluded experimental work for the most part. The formation of metal-organic complexes due to an interaction between the 2-MBT molecules and copper (metal/oxides) has also been suggested [19,22–24,34], though only a few authors have been able to validate the formation of these Cu(I)-2-MBT complexes experimentally [22–24].

The inhibiting effect of 2-MBT on the corrosion of copper in neutral chloride conditions has been discussed by several authors [21,23,25,34]. However, these works only focused on adsorption of 2-MBT on copper samples which were already covered by an air-formed native oxide film; therefore, a prolonged exposure time to 2-MBT was needed to ensure adsorption of the inhibitor. Additionally, the overall inhibiting effect of the molecule on copper corrosion was studied, but the influence of the inhibitor molecule on the initial stages of corrosion remains unclear. Lastly, the role of surface native oxides was not scrutinized in extensive detail, which is not optimal since the molecule being able to bond to the Cu(I) sites of the oxide precludes a clear characterization of the role of the Cu-2-MBT metal-organic complexes in protecting the surface from corrosive attack.

In the present work, we aim to clarify these questions by adsorbing the inhibitor on a metallic state of the copper surface and evaluating the inhibiting effect of the 2-MBT molecule on the initiation of corrosion in a near neutral chloride solution (3.5% NaCl). We also explore the role of the remnant native oxide, that subsists at the interface between the 2-MBT layer and the metallic copper substrate, on the formation of the organic inhibitor layer, its role on the formation of the metal-organic Cu-2-MBT complexes, and finally its effect on the protection of the surface. Previously, we reported on the adsorption of 2-MBT on copper in alkaline environment [19] and in a highly acidic chloride environment [20]. Each environment exhibited different mechanisms of 2-MBT adsorption, mostly due to the dominant conformer of the molecule prevalent in each environment, thione or thiolate. While the work in acidic chloride media was on the corrosion protection offered to copper by 2-MBT inhibitor, the work in alkaline media was done in absence of any corrosive species, which allowed us to determine the inhibition of anodic oxidation of copper by 2-MBT. In the near neutral chloride-containing environment of the present work, we expect an overlap of the properties observed in acidic chloride and alkaline media. This is due to the presence of both thione and thiolate form of 2-MBT [24], the passivation capability of copper in environments with a pH greater

than 5 [35], and the effect of chloride ions on the system. Thus, we can discuss how each parameter affects the bonding mechanisms between the 2-MBT molecule and the copper substrate and the corrosion inhibition by the 2-MBT organic inhibitor. Lastly, we can determine whether the metal-organic complexes protect the substrate from corrosion. The present work provides deeper insight in the understanding of the corrosion protection offered by 2-MBT to copper metal in a seawater concentration (0.5 M) of NaCl, where copper has numerous applications.

Electrochemical techniques were used to reduce the native oxide film initially present on the copper surface and subsequently adsorb the inhibitor on a metallic surface state. Surface analysis using X-ray photoelectron spectroscopy (XPS) and time-of-flight secondary ion mass spectrometry (ToF-SIMS) was used to evaluate the formation of the organic inhibitor film, its bonding mechanism to the substrate, the role of the residual oxides, and the effect of exposure time on 2-MBT adsorption. The effects of the pre-adsorbed inhibitor layer on the protection of copper against corrosion were studied using cyclic voltammetry (CV). After polarisation, the stability of the 2-MBT inhibitor layer upon anodic polarisation along with the changes induced on the surface layers were investigated by XPS.

Experimental

The polycrystalline samples were obtained from high-purity cast electrolytic tough pitch copper (ETP-Cu), as in previous work [19,20,31]. The studied surfaces were mechanically polished using silicon carbide abrasive papers down to 4000 grit, followed by diamond paste down to 0.25 µm to achieve a mirror finish surface. Samples were then cleaned ultrasonically for 5 minutes in successive baths of acetone, ethanol, and ultra-pure water (resistivity > 18.2 MΩ.cm). The cold-work layer leftover from mechanical polishing was removed by electrochemical polishing, performed using a solution of 60% H_3PO_4 at a constant voltage of 1.4 V versus a copper counter-electrode for 4 minutes [36]. The samples were finally rinsed with a 10% solution of H_3PO_4, followed by ultra-pure water, and dried using nitrogen.

The electrochemical experiments were performed using a classical three-electrode electrochemical cell. The sample was used as the working electrode, a platinum plate mesh as the counter electrode, and a saturated calomel electrode (+0.2415 V vs SHE) as the reference electrode. The working electrode area was 0.16 cm^2, delimited by an O-ring. The

experiments were performed using a Biologic SP 200 potentiostat and EC-lab collection software. The electrolytes used for the experiment were a reference 0.5 M NaCl aqueous solution of pH 5.3 ± 0.1 without the inhibitor, and a 0.5 M NaCl + 0.1 mM 2-MBT aqueous solution of pH 5.2 ± 0.1 as the solution with inhibitor. A low concentration of the 2-MBT inhibitor was used due to its limited solubility in water. The chemicals used were supplied by Sigma Aldrich and were of analytical grade and the solutions prepared with ultra-pure water.

Cathodic pre-treatment was performed on the substrates to reduce the native oxide film initially present on the surface. After immersion at the open circuit potential, the potential was swept down to the onset of hydrogen gas evolution (–0.86 V vs SHE) and then back up to the potential at which the measured current was zero (–0.16 V vs SHE), with a scan rate of 20 mV/s. This was repeated 2 more times to ensure maximum reduction of the native oxide film. The anodic polarisation tests were performed by sweeping the potential from –0.16 V vs SHE up to the initiation of corrosion, followed by reverse sweeping to –0.56 V vs SHE, and then back to –0.16 V vs SHE. The electrochemical experiments were repeated in threefold to ensure reproducibility of the results.

Surface analysis was performed after cathodic pre-treatment followed by 2-MBT adsorption on the surfaces, and in the anodically polarized state (anodic state at 0.09 V vs SHE, before initiation of corrosion). Once the relevant electrochemical state was obtained, the cell was disconnected, the samples rinsed with ultra-pure water, dried using nitrogen, and transferred within 2 minutes for analysis by XPS and ToF-SIMS.

XPS analysis was performed using a Thermo Electron Escalab 250 Xi spectrometer with a base pressure less than 10^{-10} mbar. A monochromated Al Kα X-ray source (hv = 1486.6 eV) was used with an X-ray spot size of 900 µm in diameter for the analysis. Survey spectra were recorded with a pass energy of 100 eV at a step size of 1 eV, and high-resolution spectra of the C 1s, N 1s, S 2p, O 1s, Cu 2p, Cl 2p core levels, and Cu LMM Auger transition were recorded with a pass energy of 20 eV at a step size of 0.1 eV and at 90° take-off angle. The binding energies were referred to the Fermi level of the sample. Curve fitting of the spectra was performed with the Thermo Fischer scientific software Avantage using an iterative Shirley-type background subtraction. CasaXPS software was used to decompose the Cu LMM Auger spectra. The values of the photoionization cross-sections at 1486.6 eV were taken from the Scofield database [37], the transmission function of the analyser was given by Thermo Fisher,

and the inelastic mean free paths were determined using the TPP-2M formula [38]. The estimation of the coverage and thickness of the interfacial oxide and the thickness of the 2-MBT films were calculated using the same method as in previous works, where the bi-layer model, the system of equations which were solved numerically, the values for the parameters used, along with the assumptions considered for the model have been detailed [19,20].

ToF-SIMS analysis was performed using a ToF-SIMS 5 spectrometer (IonTof – Münster Germany) with a base pressure of ~5 x 10^{-9} mbar. Data acquisition and post processing analysis were carried out using the SurfaceLab software v6.5. High current (HC) bunched mode was used for performing analysis using Bi^+ primary ions of 25 keV energy at a target current of 1.2 pA over an area of 100 x 100 µm². A bismuth beam was used to optimize the characterization of both the organic (2-MBT layer) and inorganic parts (copper oxide, copper substrate) of the interface, whereas an argon beam would be more suitable for the organic layer only. Depth profiles were obtained by interlacing analysis in static SIMS conditions with sputtering using a Cs^+ ion gun of 0.5 keV delivering a 20 nA target current over a 500 x 500 µm² area. Both ion beams were at an incidence of 45° with respect to the sample surface. They were well-aligned to ensure analysis at the centre of the sputtered crater. The acquisitions were performed in negative polarity allowing us to analyse both the organic regions and the inorganic oxide regions of the surface. The depth profiles were recorded at three separate regions on the surface of each sample to ensure reproducibility.

Results and discussion

Formation of the 2-MBT organic barrier layer

Two methods of cathodic pre-treatment were used: (a) pre-treatment in a solution of 0.5 M NaCl + 0.1 mM 2-MBT (with inhibitor), and (b) pre-treatment in a solution of 0.5 M NaCl (without inhibitor). Figure 1 shows the three CV cycles of the cathodic pre-treatment in each electrolyte with the current density measured as the potential is swept from OCP to the onset of hydrogen gas evolution and back.

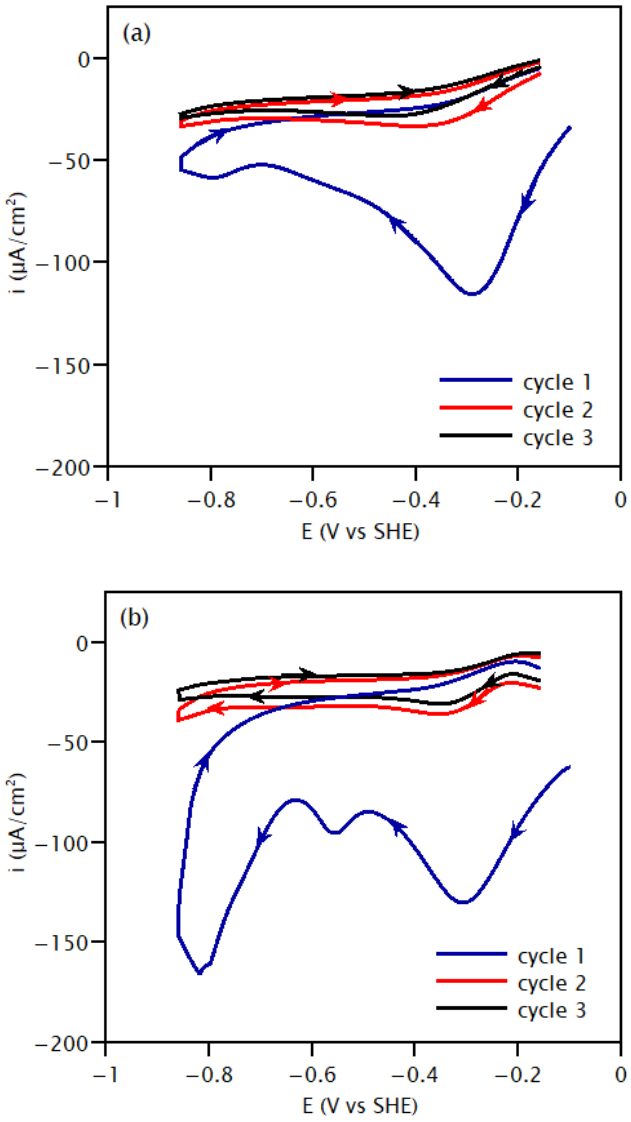

Figure 1: Cathodic pre-treatment curves obtained using cyclic voltammetry with a scan rate of 20 mV/s on copper in (a) 0.5 M NaCl + 0.1 mM 2-MBT solution (with inhibitor), and in (b) 0.5 M NaCl solution (without inhibitor). Arrowheads are added to each cycle to guide the reader's eye.

For the first cycle of the pre-treatment, a distinct cathodic peak of similar magnitude is observed at approximately –0.3 V vs SHE in both cases. This peak corresponds to the reduction of Cu(I) oxide (Cu_2O) natively formed on the Cu substrate, as seen in previous work in alkaline environment [19]. Its similar amplitude in both solutions (with/without inhibitor) suggests no major effect of the inhibitor on the cathodic reduction of the oxide in this potential range, in contrast with the marked effect observed in chloride-free alkaline environment [19]. A possible explanation is that chloride ions competitively adsorb on the oxide film surface and poison the cathodic reduction reaction of the oxide in this potential range independently of

the presence of the inhibitor. A second smaller peak is observed at –0.57 V vs SHE for the pre-treatment without inhibitor (Figure 1b) whereas only a shoulder is measured at this potential for the pre-treatment with inhibitor. The second peak for the pre-treatment with inhibitor is shifted to –0.78 V vs SHE (Figure 1a). The nature of the related cathodic reduction process remains unclear although it likely involves adsorbed chloride ions since it has not been observed in a chloride-free environment [19]. The decrease in amplitude and the negative shift observed for the pre-treatment with the inhibitor suggest an influence of the 2-MBT molecules on this process. Finally, for the pre-treatment without inhibitor (Figure 1b), the hydrogen evolution initiates at around –0.65V vs SHE. However, this is not observed for the pre-treatment with 2-MBT even until a potential of approximately –0.9 V vs SHE (Figure 1a), indicating the influence of 2-MBT also on the cathodic reaction of water reduction occurring here.

The next two cycles for both pre-treatment methods result in much lower cathodic current densities compared to the first cycle. However, we do observe that the shape of the curves is slightly different for both methods. In the case of pre-treatment without inhibitor (Figure 1b), a small but distinct peak is observed at a potential of approximately –0.3V vs SHE for the second and third cycles, reminiscent of the peak from the first cycle. This suggests that there is still some reduction of the native oxide occurring here and decreasing in amplitude with repeated cycling. This distinct peak is not observed for the pre-treatment with inhibitor (Figure 1a), where an increase in negative current density is observed and shifted negatively, however, not characteristic of a reduction peak. This suggests that the 2-MBT molecules have an inhibiting effect on the reduction of the remaining oxides, further observed in the third cycle of the pre-treatment. In the potential range negative to –0.65V vs SHE, the inhibiting effect of 2-MBT on the cathodic reaction of water reduction is confirmed in the second and third cycles with the absence of any discernible peak indicative of the reaction.

In order to characterize the reduction of the native oxides further and to study its effect on the formation of the 2-MBT inhibiting layer, surface analysis was carried out after the three cycles of pre-treatment in (a) 0.5M NaCl + 0.1 mM 2-MBT, (b) 0.5 M NaCl followed by 2 minutes exposure to the 2-MBT containing solution, and (c) 0.5 M NaCl followed by 1 hour exposure to the 2-MBT containing solution. In the latter two pre-treatment methods (without

inhibitor), the 2-MBT containing solution was introduced after the three cycles to enable the adsorption of the molecule on the substrate.

The ToF-SIMS elemental depth profiles of the resulting interfaces are presented in Figure 2 (a-c). These profiles display the intensity of the selected secondary ions in logarithmic scale vs the sputtering time in seconds. The sputtering time relates to the depth of the substrate from the topmost surface. The Cu^- and Cu_2O^- ions were selected as characteristic of the metallic substrate and Cu oxide, respectively, as previously reported [19–21]. The $C_7H_4NS_2^-$ ion corresponds to the 2-MBT organic molecule as a whole, while the C_2N^- and C_2S^- ions are representative of the 2-MBT molecular fragments of nitrogen and sulphur in interaction with the substrate. The $^{34}S^-$ and $^{37}Cl^-$ ion profiles are characteristic of the overall sulphur and chloride species, respectively. Finally, the $CuC_7H_4NS_2^-$ ions were selected as characteristic of the Cu-2-MBT interaction, both as bonding to the metallic/oxidized substrate and possible metal-organic complexes, as discussed in previous work [19]. The positions of each layer were defined by the maximum intensity of the corresponding ions with an uncertainty of 5%.

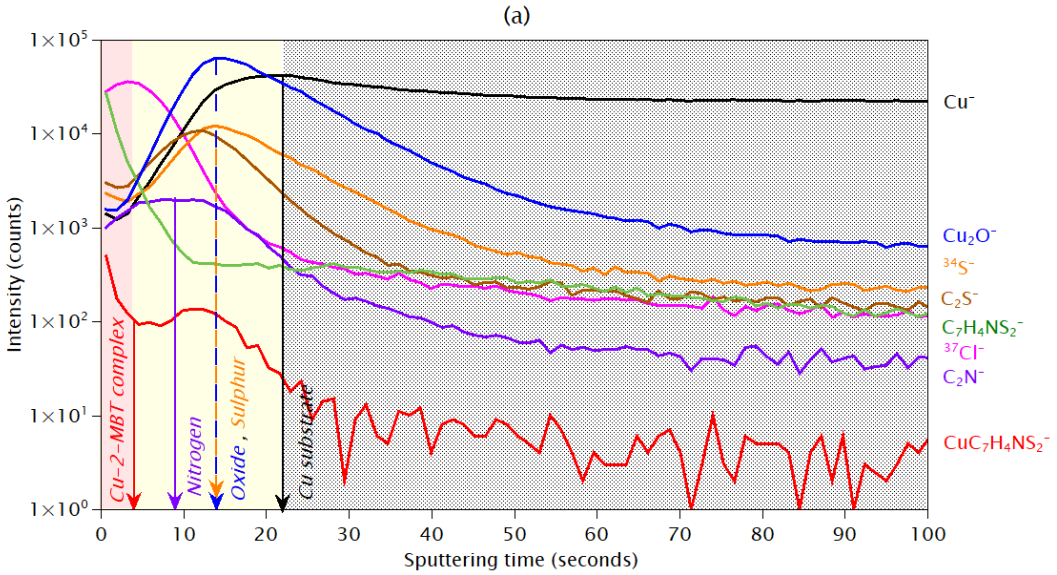

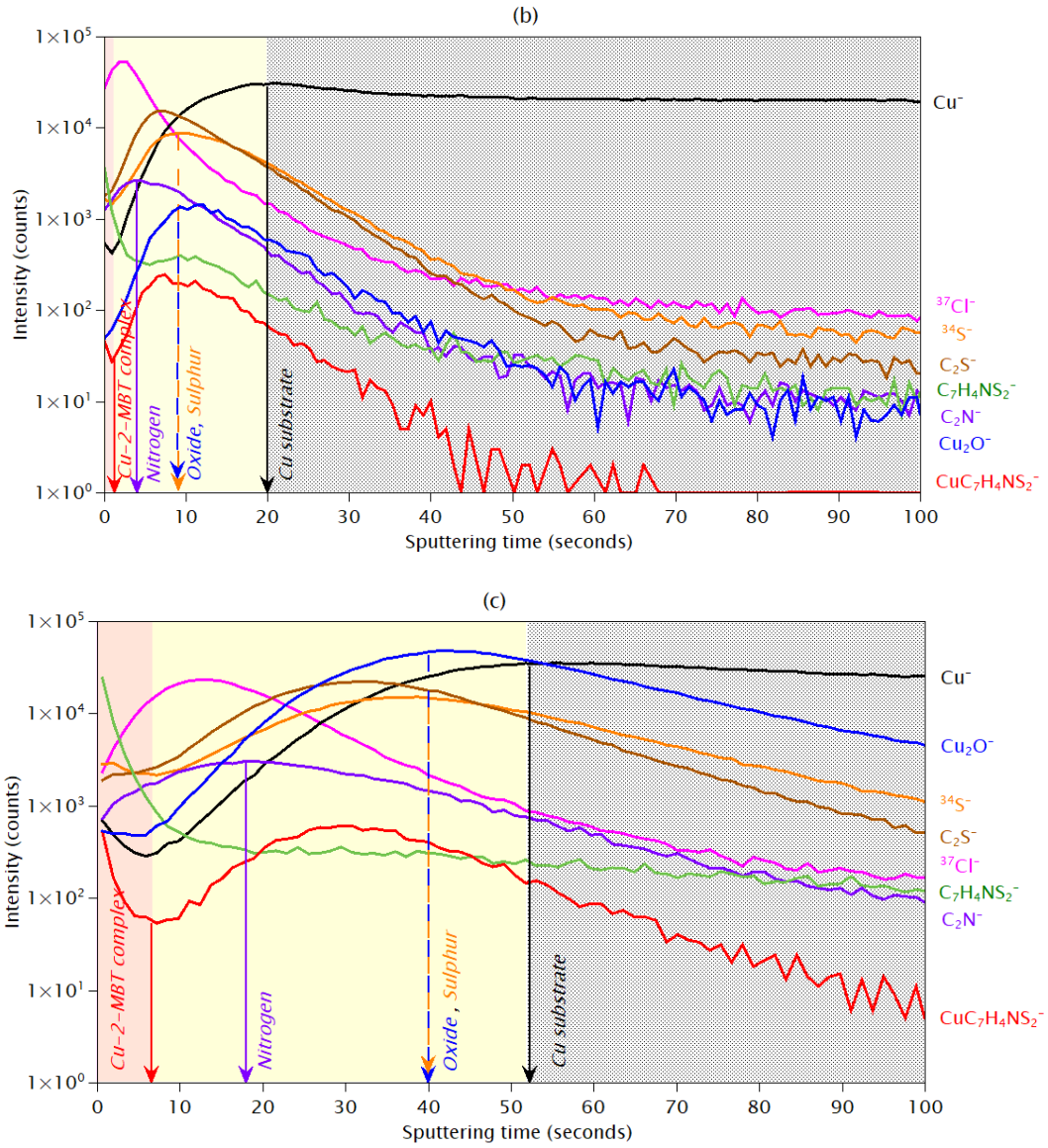

Figure 2: ToF-SIMS depth profiles for the 2-MBT/copper interfaces formed in 0.5 M NaCl solution after (a) cathodic pre-treatment in presence of 2-MBT, (b) cathodic pre-treatment in absence of 2-MBT followed by 2 minutes exposure to 2-MBT, and (c) cathodic pre-treatment in absence of 2-MBT followed by 1 hour exposure to 2-MBT.

For the depth profile obtained after cathodic pre-treatment in the presence of 2-MBT (Figure 2a), the Cu metallic substrate is reached at 22 seconds of sputtering as indicated by the maximum intensity of the Cu^- signal. Although cathodic pre-treatment was applied to the substrate, remnant oxides subsist at the interface between the metallic substrate and the 2-MBT organic layer, as indicated by the increase of the Cu_2O^- signal that reaches its maximum intensity at 14 seconds of sputtering. This is in agreement with the CV data suggesting the presence of oxide remnants after the cathodic pre-treatment in presence of the inhibitor. Considering the 2-MBT molecular fragment ion profiles, the C_2S^- ion profile peaks at a larger

depth (12 s) compared to the C_2N^- ion profile (9 s), indicating that it is most likely the sulphur atoms which bond to the substrate and/or the remnant oxides. Furthermore, the $^{34}S^-$ ion profile peaks at 14 seconds of sputtering, which endorses our claim of sulphur bonding. We also note that both the Cu_2O^- and $^{34}S^-$ ion profiles exhibit their maximum intensity at the same sputtering time of 14 seconds, suggesting that the oxides are not in the form of a homogeneous layer, but rather in the form of isolated and dispersed islands on the surface. These findings are consistent with previous work of 2-MBT adsorption on copper surfaces in acidic and alkaline media [19,20]. The ion profile of $C_7H_4NS_2^-$, characteristic of the 2-MBT molecule, shows a progressive intensity decrease from the surface up to 10 seconds of sputtering time where it reaches a minimum intensity plateau. This is associated with the formation of physisorbed multi-layers of 2-MBT on the surface, that are easily sputtered away within the initial few seconds of sputtering, as discussed in previous work [19,21].

The $CuC_7H_4NS_2^-$ ion profile in Figure 2a exhibits a more complex behaviour. A decrease in intensity is observed up to 3 seconds of sputtering followed by a shoulder centered around 11 seconds of sputtering. The shoulder is assigned to the bonding of the molecule with the substrate, whereas the initial decrease is most likely due to the formation of metal-organic complexes which are deposited on the surface, as concluded in previous work in alkaline media [19] and suggested by other authors [24]. The formation of metal-organic complexes is also attested by the shape of the Cu^- ion profile for the first 3 seconds of sputtering time which correlates to that of the $CuC_7H_4NS_2^-$ ion profile, with a small decrease observed initially. Finally, the $^{37}Cl^-$ ion profile peaks at only 3 seconds of sputtering and decreases sharply with increased sputtering time. This indicates that the chloride ions are mostly adsorbed in the outer layer followed by a limited interaction with the oxides. The effect of the chloride ions on the metallic substrate is negligible, as attested by the shape of the ion profile.

The depth profile of the substrate pre-treated in absence of 2-MBT followed by 2 minutes of exposure to 2-MBT (Figure 2b) shows a similar structure to that of the substrate pre-treated in presence of 2-MBT (Figure 2a), regarding the presence of oxide islands, the sulphur bonding to the substrate, and the physisorbed 2-MBT molecules on the surface. Although the difference in sputtering time between the peaks of the Cu^- and Cu_2O^- ion profile is similar to the previous case, i.e., 8 – 10 seconds, the intensity of the Cu_2O^- ion is lower by almost 2

orders of magnitude here. This suggests that the overall oxide quantity (thickness and coverage) is lower in the substrate pre-treated in absence of 2-MBT (Figure 2b).

The major difference between the two depth profiles relates to the $CuC_7H_4NS_2^-$ ion profile, where the initial intensity is rather weak (Figure 2b) compared to the previous case (Figure 2a). This suggests very little formation of the metal-organic complexes in this case, also seen by the lower intensity of the Cu^- ion profile for the first 2 seconds of sputtering. The rationale for this phenomenon is discussed further on. However, the inner shoulder of the $CuC_7H_4NS_2^-$ ion profile remains consistent with the previous case, indicating bonding of the molecule with the Cu substrate. The $^{37}Cl^-$ ion profile again peaks near the surface suggesting chloride ions adsorption on the surface and reduced interaction with the inner layers. Regarding the thicknesses of the interfacial oxide layer and the 2-MBT organic layer, it is difficult to conclude between the two pre-treatments since the structure of the layers and the surface roughness play an important role in the shape and the peak position of the ion depth profiles. Therefore, we leave the interpretation of the layer thicknesses by ToF-SIMS and rather estimate them using XPS analysis, as discussed further on.

For the depth profiles obtained after cathodic pre-treatment in absence of 2-MBT followed by 1 hour exposure to 2-MBT (Figure 2c), the range of sputtering time for each layer has significantly increased compared to the previous two methods of 2-MBT deposition on the substrate, by a factor of more than 2 times. This can be attributed to two main factors: the formation of a thicker 2-MBT layer and oxide islands (which we discuss further based on the XPS data), and the modification of the structure of the layers along with an increased surface roughness. Despite the changes observed regarding the range of sputtering time, the inhibitor layer and the interface oxide layer in Figure 2c are sequenced similarly to the previous two cases. The $C_7H_4NS_2^-$ ion profile shows a larger range of decrease, until 12 seconds of sputtering time, indicating a thicker outer physisorbed layer. The initial decrease of the $CuC_7H_4NS_2^-$ ion profile occurs for a longer sputtering time here, indicating increased formation of the Cu-2-MBT complexes upon a longer exposure time to the NaCl solution. This is confirmed by the Cu^- ion profile's initial decrease which coincides with that of the $CuC_7H_4NS_2^-$ ion profile.

Lastly, we observe that the $^{37}Cl^-$ ion profile exhibits its maximum intensity at approximately 12 seconds (Figure 2c), i.e. at the same sputtering time as the minimum intensity plateau of the $C_7H_4NS_2^-$ ion profile. This indicates that the chloride ions have penetrated the outer physisorbed 2-MBT layer in this substrate, unlike the previous two cases. Therefore, it is likely that the chloride ions also have an increased effect on the oxides here, caused by the prolonged exposure to the chloride containing solution. The intensity of the $^{37}Cl^-$ ion profile decreases steadily after 20 seconds of sputtering, indicating that the chloride effect is reduced at greater depths of the substrate, due to the inner 2-MBT layer impeding its pathways to the metal substrate and thus protecting it.

The Cu LMM Auger spectra obtained after cathodic pre-treatment for the three electrochemical conditions of interface formation are shown in Figure 3(a-c). They include the contributions of the Cu(0) and Cu(I) components corresponding to copper metal and copper oxide, respectively. The decomposition was done by least square fitting, using as components the 2 line-shapes measured, in same analytical conditions, on metallic copper and on a Cu_2O thick film, like previously done [18,20,39,40].

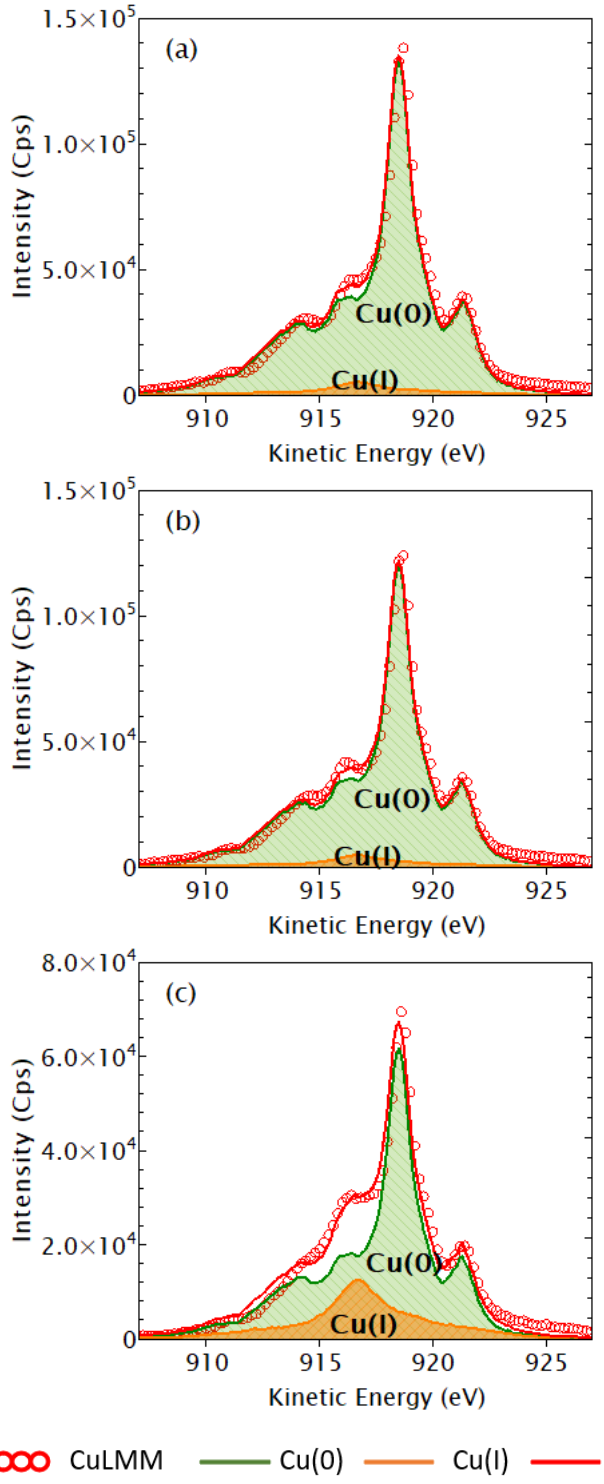

Figure 3: Cu LMM Auger spectra for the 2-MBT/copper interfaces formed in 0.5 M NaCl solution after (a) cathodic pre-treatment in the presence of 2-MBT, (b) cathodic pre-treatment in the absence of 2-MBT followed by 2 minutes exposure to 2-MBT, and (c) cathodic pre-treatment in the absence of 2-MBT followed by 1 hour exposure to 2-MBT.

It is observed that in the case of pre-treatment with 2-MBT (Figure 3a) and the pre-treatment without 2-MBT followed by 2 minutes exposure to 2-MBT (Figure 3b), the amount of oxides that subsist is very small. The Cu(I)/Cu(0) intensity ratio determined for the substrate pre-

treated with 2-MBT was 0.06 ± 0.01, whereas the ratio of the substrate pre-treated without 2-MBT followed by 2 minutes exposure to 2-MBT was 0.05 ± 0.01. This indicates that both pre-treatment methods are quite effective in reducing the native oxides present initially on the surface. Although the changes are minimal between the two pre-treatment methods, the data are in agreement with the ToF-SIMS depth profiles presented earlier in Figure 2(a-b), where the interfacial oxide layer is quite similar for both cases based on the sputtering time, but slightly different in terms of overall oxide intensity.

Despite the effectiveness of the pre-treatment methods, we observe that when the exposure time to 2-MBT is increased to 1 hour after pre-treatment in the absence of 2-MBT (Figure 3c), the quantity of the Cu(I) ions increases drastically compared to when the exposure time was only 2 minutes. The Cu(I)/Cu(0) intensity ratio determined here was 0.28 ± 0.01, which is a significant increase compared to the two cases observed earlier. This indicates that during the extended exposure time, some regions of the surface, which were most likely uncovered by the 2-MBT molecules, were further oxidized to form Cu(I) ions.

In previous work [19], it was suggested that the metal-organic complexes formed by the Cu(I) ions and 2-MBT molecules could also contribute to the Cu(I) intensity. Given that we observe the presence of these complexes from the ToF-SIMS depth profiles (Figure 2c), it is likely that the increased Cu(I) intensity observed in Figure 3 (c) could contain some contribution from these metal-organic complexes.

The normalised XPS spectra for the C 1s, N 1s, and S 2p core levels obtained after cathodic pre-treatment in the three conditions are presented in Figure 4. Spectral decomposition was performed using the parameters of the peak components defined in previous works [19,20]. The uncertainty for the binding energy (BE) values and the full widths at half maximum (FWHM) are estimated to be ± 0.1 eV.

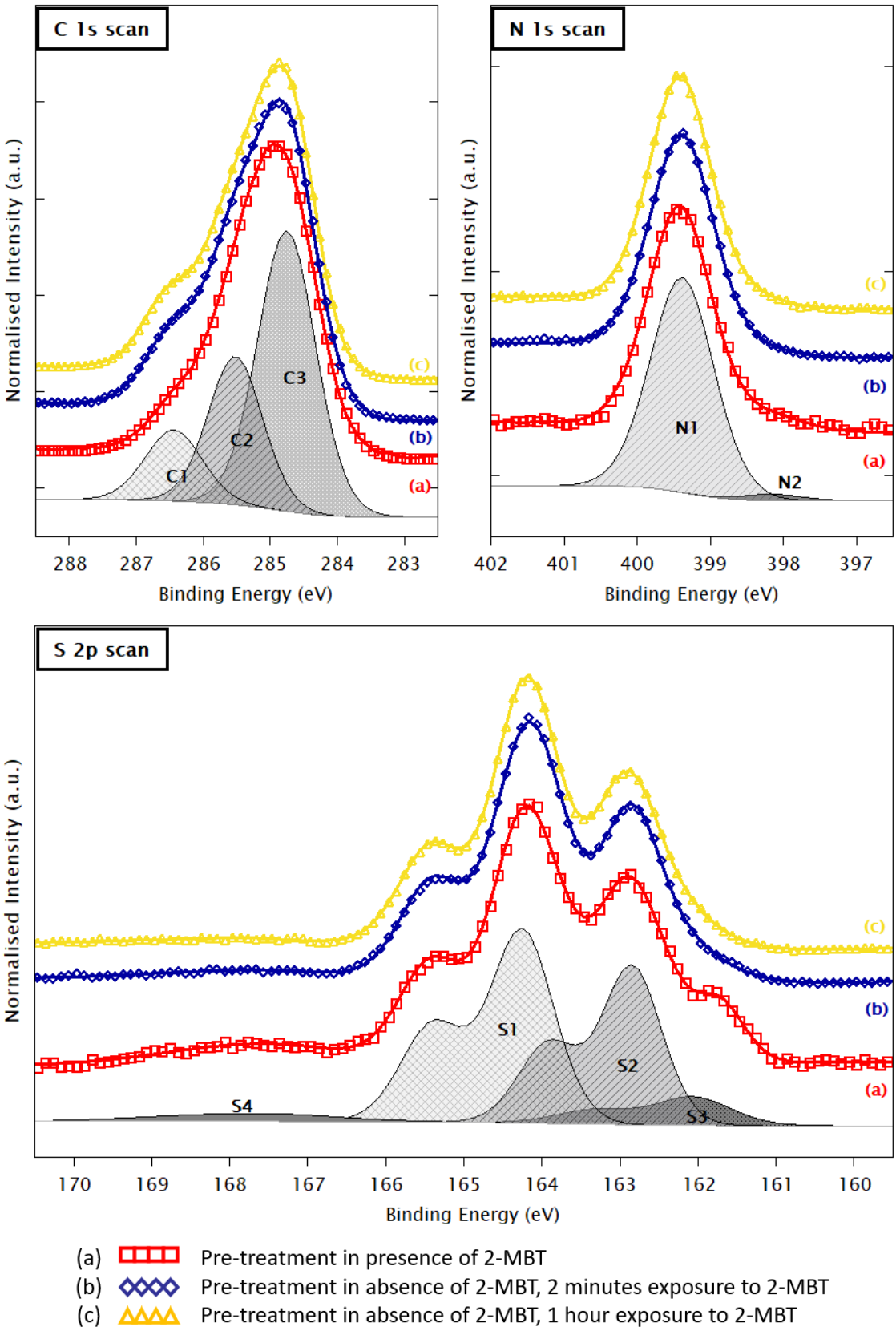

Figure 4: Normalised XPS C 1s, N 1s, and S 2p core level spectra for the 2-MBT/copper interfaces formed in 0.5 M NaCl solution after cathodic pre-treatment in (a) presence of 2-MBT, (b) absence of 2-MBT followed by 2 minutes exposure to 2-MBT, and (c) absence of 2-MBT followed by 1 hour exposure to 2-MBT. The symbols represent the experimental data and

the corresponding coloured lines represent the fitted curves. The decompositions are shown for spectra (b).

The C 1s spectra were decomposed into three chemical states. These components are C1 at 286.6 eV assigned to the C=S bonds, C2 at 285.6 eV for the C–S and C–N bonds, and finally C3 at 284.8 eV associated to the C–C and C–H bonds [16,20]. The ratio of 1:2:4 measured between these three components reflects the 7 carbon atoms from the 2-MBT molecule in their respective chemical states. This was also measured in previous work on 2-MBT adsorption on copper from vapour phase and liquid phase [16,17,19–21]. It is observed that for the substrate pre-treated in presence of 2-MBT, the shoulder corresponding to the C1 peak is less marked compared to the two substrates pre-treated in absence of 2-MBT. This is due to the slightly larger FWHM (+0.1 eV) of the three carbon components here, most likely caused by a change in the structure of the 2-MBT organic film formed on the substrate pre-treated in the 2-MBT-containing solution.

The N 1s spectra exhibits two components: N1 at 399.4 eV and N2 at 398.2 eV. These components correspond to N not bonded to Cu for N1 and N directly bonded to metallic Cu for the N2 component, as observed previously for adsorption from the vapour phase and in an aqueous alkaline environment [16,19]. Like in previous work, the fraction of N2 is small, approximately 7% for the substrate pre-treated in presence of 2-MBT and less than 3% for the substrates pre-treated in the absence of 2-MBT, indicating that the bonding between the metallic substrate and nitrogen atoms of the molecule is limited and is not the major bonding mechanism between the metal and the 2-MBT molecule.

The S 2p spectra were decomposed using $2p_{3/2}$ – $2p_{1/2}$ spin-orbit doublets with a branching ratio of 0.5 and splitting of 1.18 eV. The S $2p_{3/2}$ chemical states at 164.2 eV (S1) and 162.8 eV (S2) correspond to the endocyclic and exocyclic sulphur atoms from the 2-MBT molecule, respectively [16–21]. Both these components are not directly bonded to metallic Cu, rather, they result from an interaction between the molecule and the copper oxides, and/or from the formation of 2-MBT multi-layers, and/or from the formation of Cu-2-MBT complexes. The S $2p_{3/2}$ component observed at 161.9 eV (S3) was associated to sulphur bonded directly to metallic Cu [16,17,19,20,41]. Previous work has shown that this component can arise from 2-MBT molecules in their entirety bonding via sulphur to the metallic substrate and from free dissociated sulphur bonding to the metallic substrate [16,19,20]. The presence of the S3

component confirms our analysis from the ToF-SIMS depth profiles that the interfacial oxides are not in a homogeneous layer, but rather distributed as islands on the surface. From the atomic ratio between the sulphur and nitrogen intensities, it was established that there is indeed an excess of sulphur (approximately 15%) for all three substrates, compared to the theoretical value of 2:1 for the S:N ratio, confirming the presence of free dissociated sulphur atoms. Lastly, a fourth sulphur component (S4) at 167.6 ± 0.3 eV was observed for all three cases with a FWHM of 2.4 ± 0.2 eV. This component is representative of sulphate and/or sulphone groups that are likely formed by an interaction of sulphur from the 2-MBT molecules with oxygen, resulting in sulphur atoms doubly bonded to two oxygen atoms each [42]. However, this component represents a very small fraction of the overall sulphur intensity, less than 5% for all three S 2p spectra, and is considered inconsequential for quantitative analysis.

We observe that the line-shapes of the S 2p spectra for the interfaces prepared by pre-treatment in absence of 2-MBT are similar for 2 minutes and 1 hour exposure to 2-MBT, with negligible changes in relative intensities between the components. However, a distinct difference is observed for the line-shape of the S 2p spectrum for the interface prepared by pre-treatment in presence of 2-MBT, with a marked shoulder at the position of the S3 component. This is due to the slightly increased relative intensity of the S3 component here. Further analysis of the sulphur components by determination of atomic ratios revealed that this relative increase in the S3 component originates from a slight decrease in the relative intensity of the S1 component (endocyclic sulphur). Therefore, for the substrate pre-treated in presence of 2-MBT (Figure 4, spectra a) the S3 originates both from the endocyclic and exocyclic sulphur, whereas for the substrates pre-treated in the absence of 2-MBT (Figure 4, spectra b and c), the S3 originates mainly from the exocyclic sulphur. As mentioned earlier, this is most likely due to the different bonding mechanisms and the structure of the organic film formed, possibly due to the presence and influence of the oxide remnants on the metallic substrate surface.

The Cl 2p spectra (see Figure S1 in supplementary information (SI)) exhibits only one component corresponding to adsorbed chlorine on the surface at a BE of 198.3 eV (Cl $2p_{3/2}$), as seen in previous work [19,20]. However, due to the low signal to noise ratio for the Cl 2p spectra, we cannot completely exclude the possibility of the presence of CuCl at a BE of 199 eV. Nevertheless, the intensity of the Cl peaks is very low, indicating minimal interaction with

the copper substrate, as indicated by the ToF-SIMS depth profiles presented above. Lastly, the O 1s spectra (see Figure S2 in SI) are also consistent with previous work [19,20], with three components observed, corresponding to metal oxides (Cu_2O) at a binding energy of 530 eV, hydroxides at 531.4 eV, and oxygen from water adsorbed on the surface at 532.9 eV.

To evaluate the differences in organic 2-MBT layers and interfacial oxide layers formed on the copper substrate by each pre-treatment method, the thickness and coverage of the films were estimated using the same bi-layer model as previously described [19,20], and shown in SI (Figure S3). The results are presented in Table 1. The uncertainty on the coverage of the oxide islands is estimated to be 10% and that on the thickness of the films to be ± 0.2 nm. The equivalent thicknesses are also estimated for the purpose of a straightforward comparison between the pre-treatment methods.

Table 1: Thickness and coverage of the interfacial copper oxide islands and the 2-MBT inhibitor layers formed on copper in 0.5 M NaCl solution depending on pre-treatment as listed. The equivalent thicknesses are tabulated by weighting the estimated thickness of each layer with its coverage. The uncertainty on the coverage is estimated to be ± 10% and the uncertainty on the thicknesses is estimated to be ± 0.2 nm.

	Conditions of interface formation	Coverage of Cu_2O islands (%)	Thickness of Cu_2O islands (nm)	Equivalent thickness of Cu_2O (nm)	Thickness of 2-MBT layer above oxides (nm)	Thickness of 2-MBT layer above metallic Cu (nm)	Equivalent thickness of 2-MBT layer (nm)
a	Pre-treatment with 2-MBT	83	0.3	0.3	0.7	1.0	0.7
b	Pre-treatment w/o 2-MBT, 2 mins exposure to 2-MBT	58	0.2	0.1	1.8	2.0	1.9
c	Pre-treatment w/o 2-MBT, 1 hr exposure to 2-MBT	46	0.9	0.4	1.7	2.6	2.2

It is observed that for the pre-treatment in presence of 2-MBT, even though the thickness of the oxide islands is quite low, in the order of one monolayer of oxide, the coverage of the oxide islands on the surface is quite high. This is in agreement with the results from the ToF-SIMS depth profiles in Figure 2a. This indicates that although this pre-treatment does reduce

most of the native oxides in terms of thickness, it is not effective enough to clear the surface of the oxides. Therefore, the bonding between the metallic substrate and sulphur from the 2-MBT molecule is limited to only 17% of the surface. Regarding the 2-MBT layer, it is only 0.7 nm in equivalent thickness. Assuming that the molecule is bonded in an upright position on the surface, this corresponds to only one monolayer of adsorbed molecules, since the height of the 2-MBT molecule is 0.8 nm [43]. However, we cannot discount the fact that the molecules may adsorb in different orientations on the surface, thus obtaining a second layer of the molecules (multi-layer film). Additionally, it is important to note that we have considered a model which assumes homogeneity of the layers on the surface, which is not necessarily the condition of the substrate. Therefore, we could have regions of multi-layers and regions of monolayers on the substrate surface.

For the pre-treatment without 2-MBT followed by 2 minutes of exposure to 2-MBT, Table 1 shows that the coverage of the oxide islands is significantly less (58%), and their thickness is approximately one monolayer, demonstrating that pre-treatment in absence of 2-MBT results in a better reduction of the native oxides, as seen in acidic and alkaline media too [19,20]. The lower oxide islands coverage also indicates a higher coverage of the 2-MBT molecules bonded to the metallic substrate, indicating that the adsorption of 2-MBT is favoured by direct bonding to the substrate, i.e., in the absence of oxides on the surface. In addition, the thickness of the 2-MBT layer is significantly higher in this case compared to when the pre-treatment was done in presence of 2-MBT. This suggests that the structure of the first 2-MBT adsorbed layer formed here is better suited for the adsorption of subsequent layers of the molecule even with a short exposure time.

As the overall quantity of interfacial oxides is lower after pre-treatment without 2-MBT, we conclude that the formation of the metal-organic complexes on this substrate (pre-treated without 2-MBT, 2 minutes exposure to 2-MBT) is significantly less, as indicated by the depth profiles in Figure 2b. This implies that the Cu-2-MBT complexes are composed of Cu(I) ions which originate from the metal oxides (Cu_2O) present [24]. Cathodic reduction in the absence of 2-MBT would result in less capture of the released Cu(I) ions by the organic molecules and therefore in less complexes being formed.

When the exposure time to the 2-MBT solution with NaCl is increased to 1 hour, the coverage of the oxide islands decreases slightly, however, their thickness increases drastically (about

four times compared to 2 minutes exposure with the same pre-treatment method, Table 1). This phenomenon is in line with the results of the Cu LMM Auger spectra in Figure 3c, where the increase in the Cu(I) ions was considerable after 1 hour exposure to the 2-MBT containing NaCl solution. This reveals that the oxide islands may not be well protected by the 2-MBT layer, which is likely defective in certain regions and not completely homogenous and covering as we assume it to be, thus enabling the growth of the oxide islands over time in a near neutral solution. The defects formed in the 2-MBT layer are most likely induced by the Cl^- ions present in the environment, which compete for adsorption with 2-MBT. It is important to note that we cannot rule out a slight oxidation of the surface in the defective regions of the 2-MBT barrier layer or in regions that may not be covered by the 2-MBT layer during transfer of the samples through air. Regardless, we do observe that the thickness of the 2-MBT layer has increased over time as reflected by an increase of approximately 0.3 nm of equivalent thickness compared to the shorter exposure time. However, this increase in 2-MBT layer thickness could also possibly be due to the increased formation and subsequent deposition of the Cu-2-MBT complexes on the surface, as indicated by the depth profiles in Figure 2c. The increase in thickness of the oxide islands could promote the complex formation, owing to formation of Cu(I) ions which interact with the adsorbed 2-MBT molecules.

Inhibition of oxidation and corrosion

Cyclic voltammetry was applied after preparation of the interface by the pre-treatment methods discussed above and in a reference 0.5 M NaCl solution in order to study the effect of 2-MBT on the inhibition of oxide growth and corrosion upon anodic polarisation. The CVs are presented in Figure 5, with the current density measured as the potential is swept up to the value where initiation of corrosion is observed, down to the point of hydrogen gas evolution, and back to the initial starting point. The corresponding anodic and cathodic charge densities, determined from each curve by integrating the current density over time, are presented in Table 2.

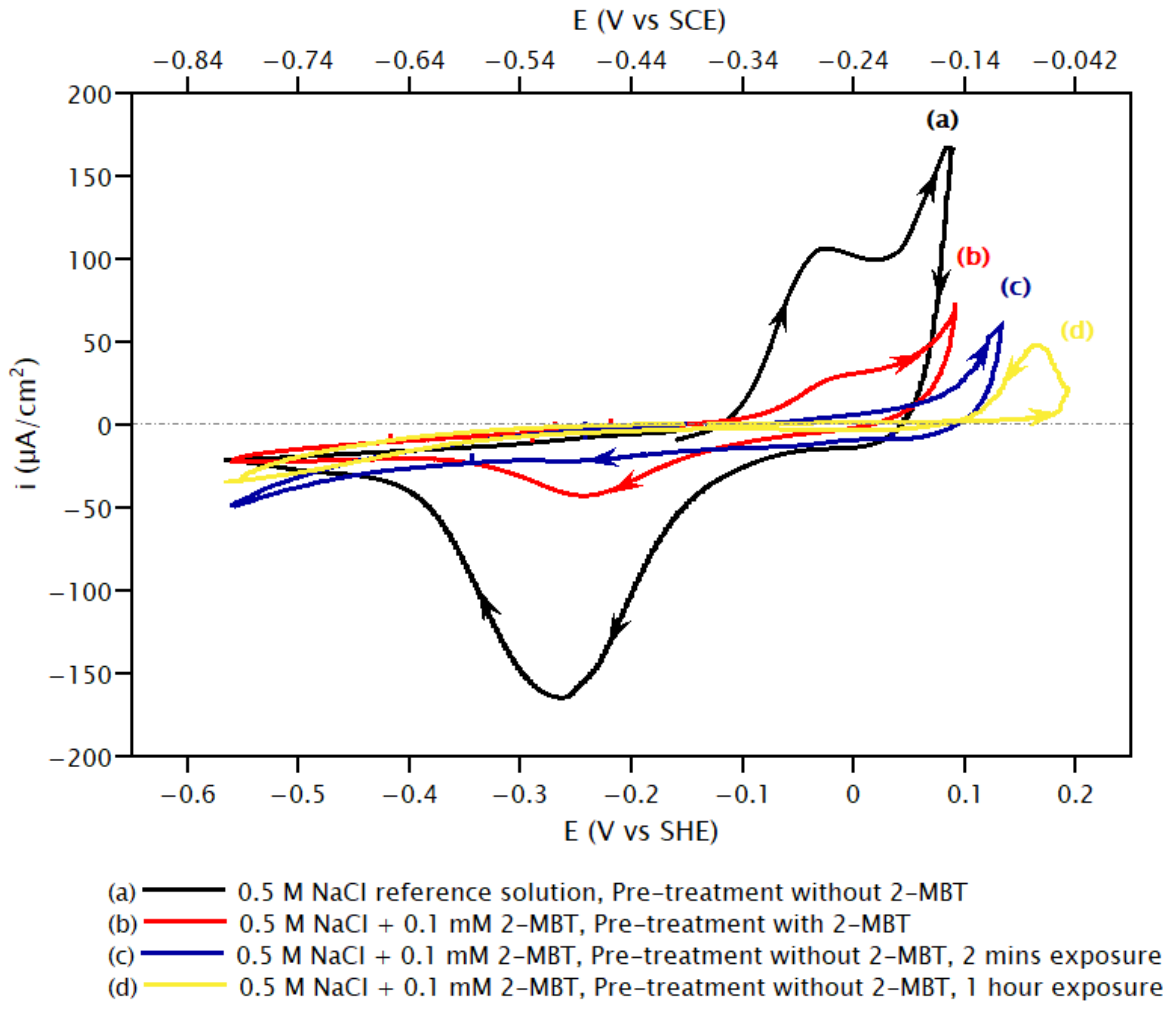

Figure 5: Cyclic voltammograms of copper showing anodic oxidation and subsequent initiation of corrosion in the absence or presence of 2-MBT in the 0.5 M NaCl electrolyte after cathodic pre-treatment as specified. Scan rate is 20 mV/s. Arrowheads are added to each cycle to guide the reader's eye.

In the 0.5 M NaCl reference solution (black curve in Figure 5), oxidation of the sample (Cu(0) to Cu(I)) initiates immediately upon anodic polarisation, with a peak at –0.02 V vs SHE, followed by the initiation of corrosion at 0.05 V vs SHE, indicated by the sharp rise in current density. Additional experiments revealed that continuous increase was observed for increased anodic polarization, with the anodic current density reaching up to 25000 µA/cm² at 0.5 V vs SHE (from ~100 µA/cm² at 0.05 V vs SHE), thus corroding the surface severely. However, since we are investigating the initiation of corrosion and its inhibition in this work, we have limited the potential accordingly.

During the reverse scan, a single cathodic peak is observed at –0.27 V vs SHE, which corresponds to the reduction of Cu(I) to Cu(0). From Table 2, we observe that the difference,

if any considering the error, between the anodic and cathodic charge densities for this experiment is very small, indicating that most, if not all, of the Cu(I) ions formed during the anodic branch of the cycle have been reduced during the cathodic sweep. Using Faraday's law [44], the equivalent thickness of copper metal reversibly consumed in this experiment is 0.86 ± 0.04 nm, using the anodic charge density where the molar volume of copper metal is 7.1 cm^3/mol and the number of electrons exchanged per copper atom is 1. Assuming the formation of a homogeneous film of Cu(I) oxide, the equivalent thickness of grown Cu_2O is estimated to be 1.41 ± 0.06 nm, using the cathodic charge density where the molar volume of Cu_2O is 23.9 cm^3/mol and the number of electrons exchanged per Cu_2O molecule is 2, which is similar to that formed in Cl-free alkaline solution in the potential range of Cu(I) oxidation (1.55 ± 0.01 nm) [19].

Table 2: Charge densities (anodic and cathodic) determined from the cyclic voltammetry tests by integrating the current densities with time.

	Electrolyte used for CV, Pre-treatment condition	Anodic charge (μC/cm²)	Cathodic charge (μC/cm²)
a	0.5 M NaCl ref. solution Pre-treatment without 2-MBT	1175 ± 60	1141 ± 47
b	0.5 M NaCl + 0.1 mM 2-MBT Pre-treatment with 2-MBT	282 ± 22	247 ± 11
c	0.5 M NaCl + 0.1 mM 2-MBT Pre-treatment without 2-MBT, 2 minutes exposure to 2-MBT	55 ± 1	39 ± 1
d	0.5 M NaCl + 0.1 mM 2-MBT Pre-treatment without 2-MBT, 1 hour exposure to 2-MBT	23 ± 1	14 ± 1

When polarisation was carried out on the interface prepared by cathodic pre-treatment in presence of 2-MBT (red curve in Figure 5), a much lower anodic current density was observed, as evident from the significantly smaller anodic peak at –0.02 V vs SHE, resulting in an anodic charge density that is approximately 4 times less compared to that in the reference solution (Table 2). This suggests that the 2-MBT layer is effective in reducing the anodic oxidation of the substrate, as seen in previous work in alkaline environment [19]. However, this 2-MBT layer is likely defective in certain regions and not entirely effective in blocking the oxidation

process, as indicated by the presence of the anodic peak. Assuming that the anodic and cathodic peaks relate to the formation and subsequent reduction of Cu(I) oxide, the equivalent thickness of grown Cu_2O estimated from the cathodic charge density is 0.31 ± 0.01 nm, which is significantly lower than the one obtained for the reference solution (4.5 times lower). Since we cannot confirm that the anodic charge corresponds only to Cu_2O formation and the cathodic charge to its reduction at this point, it is analysed by XPS further on.

The initiation of corrosion, indicated by the sharp rise in anodic current density, occurs at 0.05 V vs SHE (red curve in Figure 5), like in the previous case where there was no 2-MBT. This confirms our hypothesis that the organic inhibitor layer is defective and not protective enough against corrosion initiation, despite its inhibition of the rate of oxidation. This is most likely due to the extensive coverage of native oxides on the surface (Table 1), which precludes a more protective direct bonding between the 2-MBT molecules and the metallic substrate. Additionally, the low thickness of the 2-MBT barrier layer could also play a role here in the attack of the copper substrate, since a thinner layer is more easily penetrated by the aggressive chloride ions.

For the CVs performed after pre-treatment in absence of 2-MBT followed by 2 minutes exposure to 2-MBT (blue curve in Figure 5), there is no oxidation peak observed indicating that the 2-MBT layer better protects the metallic surface from anodic oxidation. This is also attested by the fact that the anodic charge density is approximately 21 times lower than in the reference solution and 5 times lower than after pre-treatment in presence of 2-MBT (Table 2). Additionally, the initiation of corrosion is shifted to a more positive potential, 0.1 V vs SHE, indicating that the thicker 2-MBT layer formed in these conditions (Table 1) does protect the surface from corrosion. In the reverse scan (cathodic sweep), no reduction peak is observed, which is consistent with the absence of an oxidation peak during the anodic branch of the cycle.

After longer exposure time (1 hour) to 2-MBT following pre-treatment in the absence of the inhibitor (yellow curve in Figure 5), there is a further decrease in anodic charge density by a factor of 2.4 compared to 2 minutes exposure (Table 2). This suggests that the increased coverage of metallic copper by 2-MBT and increase in overall 2-MBT layer thickness (Table 1) is more effective in hindering the oxidation reactions occurring during polarisation. We also observe a further shift in the initiation of corrosion potential to 0.17 V vs SHE. This shift

demonstrates that longer exposure times to the inhibitor does aid in the formation of a better and more effective barrier layer against corrosion.

In order to evaluate the effects of anodic polarisation on the 2-MBT organic layers and interfacial oxide layers initially formed on the copper substrates pre-treated with 2-MBT or without 2-MBT followed by 1 hour exposure to 2-MBT, XPS analysis was carried out after polarisation up to the potential of 0.09V vs SHE (i.e., before initiation of corrosion). Since the differences in the elemental core level spectra, before and after polarisation, were not apparent in terms of line-shape and relative intensities, we discuss hereafter the thickness and coverage of the oxide islands and 2-MBT layers estimated using the bi-layer model used earlier (Table 3). These values are compared to the thickness and coverage values obtained after the various cathodic pre-treatment methods in reduced state, given in Table 1.

Table 3: Thickness and coverage of the interfacial copper oxide islands and the 2-MBT inhibitor layers formed in 0.5 M NaCl solution after anodic polarization of the copper substrates pre-treated in (a) presence of 2-MBT, and (b) absence of 2-MBT followed by 1 hour of exposure to 2-MBT. Uncertainties on coverage and thickness are estimated to be ± 10% and ± 0.2 nm, respectively.

	Conditions of interface formation	Coverage of Cu_2O islands (%)	Thickness of Cu_2O islands (nm)	Equivalent thickness of Cu_2O (nm)	Thickness of 2-MBT layer above oxides (nm)	Thickness of 2-MBT layer above metallic Cu (nm)	Equivalent thickness of 2-MBT layer (nm)
a	Pre-treatment with 2-MBT	60	0.3	0.2	1.2	1.5	1.3
b	Pre-treatment w/o 2-MBT, 1 hr exposure to 2-MBT	58	0.7	0.4	1.7	2.4	2.0

For the pre-treatment in presence of 2-MBT, the coverage of the oxide islands has reduced significantly, from 83 to 60%, when compared to before anodic polarisation (Table 1). However, the thickness of these oxide islands (0.3 nm) remains the same considering the uncertainty. A possible explanation is that the coverage of the oxide islands reported in Table 1 from analysis prior to polarisation was overestimated, possibly due to oxidation of the sample in regions not covered by the defective 2-MBT layer during transfer of the samples

through air. Upon anodic polarisation, the Cu atoms in these uncovered metallic substrate regions would oxidize and bond with 2-MBT molecules, which is why a lower coverage of the oxide islands is observed here. Since the equivalent thickness of the interfacial oxide has not increased upon polarisation, it is implied that the anodic peak observed for the CV performed after pre-treatment in presence of 2-MBT (blue curve in Figure 5) does not in-fact relate to the formation of Cu(I) oxide, since the growth of the oxide film was estimated to be a thickness of 0.31 ± 0.01 nm from the cyclic voltammetry tests. Therefore, the formation of the Cu(I) ions observed from the anodic peak would correspond to the formation of Cu(I)-2-MBT metal organic complexes, as seen in previous work in alkaline environment [19]. This could also be the other possibility for the reduced coverage of oxide islands, where the most reactive Cu(I) ions from the oxide islands would preferably bind to 2-MBT molecules by a conversion reaction to form metal organic complexes induced by anodic polarization. The formation of metal organic complexes is also reflected by a significant increase in equivalent thickness of the 2-MBT layer after polarisation, from 0.7 to 1.3 nm as observed in Table 3. Regardless of their formation mechanism, it is important to note that the Cu-2-MBT complexes formed do not block the initiation of corrosion, as indicated by the similar potentials of corrosion initiation observed for the CV performed in the reference NaCl solution and for the substrate pre-treated in presence of 2-MBT (Figure 5).

In the case of pre-treatment without 2-MBT followed by 1 hour exposure to the inhibitor, the coverage of the oxide islands has increased (from 46 to 58%) compared to before polarisation and their thickness slightly decreased (from 0.9 to 0.7 nm), which results in an equivalent thickness that is unchanged (0.4 nm, Table 3). A first possibility to explain this phenomenon is that the reduction in oxide island thickness would be due to the chloride ions promoting the local thinning of the oxide islands, a mechanism proposed for the breakdown of passive oxide layers [1,11]. In this case, the coverage increase of the oxide islands could be due to the oxidation of the substrate during transfer of the sample through air in the new regions exposed by the chloride-induced dissolution of the oxide islands. Another more likely explanation is that since the equivalent thickness remains the same before and after polarisation, the changes observed for the coverage and thickness of the oxide islands merely result from the uncertainty of the estimated values and the other limitations of the model, such as the assumption of homogeneity for the thickness and coverage of the layers. This is

supported by the fact that during the anodic branch of the cyclic voltammetry test, negligible anodic current density is measured indicating little to no oxidation occurring on the substrate surface. This is due to the better protection provided by the initially thicker deposited 2-MBT layer here than on the interface pre-treated in the presence of the inhibitor.

As for the 2-MBT layer, a decreasing trend in equivalent thickness (from 2.2 to 2.0 nm (Table 3)) is suggested after polarisation. Although the local thinning process is hypothesised for oxide films on metal surfaces [1], we assume that chloride ions would have a similar effect on the 2-MBT organic layer in order to initiate corrosion on the substrate (Figure 5, curve d), thus reducing the thickness of the 2-MBT layer. However, this cannot be ascertained with our analysis methods and remains a hypothesis.

Influence of environment on the adsorption of 2-MBT

In previous work [19,20], the bonding mechanisms between the 2-MBT molecule and the copper substrate were shown to be influenced by the pH which dictates the dominant conformer of the 2-MBT molecule. Additionally, the presence and quantities of other species, such as surface oxides and chlorides, were also shown to play an important role in the bonding mechanisms and the protective properties of the organic barrier layer. Based on the adsorption mechanism of 2-MBT on copper in an acidic chloride environment and in an alkaline environment (chloride-free), we can evaluate how each individual parameter affects and changes 2-MBT adsorption on copper surfaces in a near neutral chloride environment.

The various conformers of the 2-MBT molecule - thione, thiol, and thiolate forms - are shown in Figure 6. It has been found that the thione form of the molecule is more stable over the thiol form in both solid and vapour phase [45]. In liquid environments, the dominant conformer depends on both the type of solvent and the pH of the environment. In acidic environments, the thione form is the dominant conformer of the molecule, whereas the thiolate form (ionized thiol conformer) is the dominant one in alkaline environments [24,46]. In environments where the pH is between 4 and 9, the thione and thiolate forms both co-exist [24]. Therefore, the mechanisms of bonding between the 2-MBT molecules and the copper substrate can vary based on the pH of the environment.

In an acidic chloride environment of pH between 2 to 2.5 (2-MBT thione form, Figure 6a), the 2-MBT molecules bond to the metallic substrate only by the sulphur atoms [20]. The

molecules also most likely interact with the residual native oxide-covered surface by the sulphur atoms, as suggested by ToF-SIMS depth profiling. The thickness of the residual islands of native oxide was relatively low (0.2 – 0.4 nm), even when the surfaces were pre-treated in presence of 2-MBT, mostly due to the instability of the oxide layer at pH levels lower than 5. This relatively low amount of interfacial oxide enhanced the adsorption of the 2-MBT molecules on the surface, eventually leading to thicker organic layers ranging from 1 to 2.2 nm in equivalent thickness of 2-MBT for surfaces pre-treated with and without 2-MBT, respectively. Although the chloride ions are expected to strongly interact with the surface, this was not observed in the acidic environment [20]. The first reason for this lack of chloride effect in the strongly acidic environment is that since most of the effects observed relate to the low pH of the electrolyte and the dominant thione conformer of the inhibitor, the effect of the chloride ions is relatively weaker and therefore masked by the strong pH effect. The second reason is that the bonding between the thione conformer of the 2-MBT molecules and the metallic substrate is rather strong and the 2-MBT layer densely covers the entire surface, including the residual oxidized regions as confirmed by DFT modelling [32,33], thus hindering the penetration of the chloride ions.

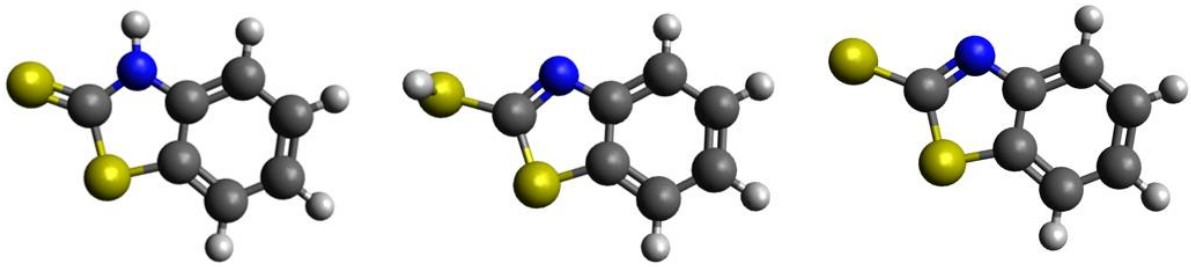

Figure 6: Models illustrating the various conformers of the 2-MBT molecule ($C_7H_5NS_2$) (a) thione form, (b) thiol form, and (c) thiolate form. The yellow atoms represent the sulphur, the blue atoms represent the nitrogen, the grey atoms represent the carbon, and the white atoms represent the hydrogen atoms in the molecule.

On the other hand, in an alkaline environment of pH between 13 to 14, the thiolate form of the 2-MBT molecule (Figure 6c) is dominant [24,46]. Here, bonding between the nitrogen atoms of the inhibitor molecules and the metallic copper substrate was observed in addition to bonding via the sulphur atoms [19], like in the present work. Although the fraction of nitrogen bonding, in both alkaline and neutral chloride conditions, is rather low compared to

that of sulphur bonding, it was a feature that was not observed in acidic environment [20]. Additionally, the formation of Cu-2-MBT metal-organic complexes was observed from the ToF-SIMS depth profiles in the alkaline environment, especially when the surfaces were pre-treated with 2-MBT in the NaOH solution [19], also similar to the present conditions. This too was not seen in experiments performed in acidic media [20]. It was proposed that the Cu(I) ions, released during the cathodic reduction (pre-treatment) process of the native oxide-covered surface or subsequently formed upon anodic polarisation, interact with the 2-MBT molecules to form these complexes which deposited on the surface of the organic layer [19].This was supported by the much thicker 2-MBT layer (2.7 – 3 nm) formed on surfaces pre-treated with 2-MBT, where the remaining interfacial oxide was relatively thicker (0.5 – 0.6 nm). Meanwhile, the surfaces pre-treated in absence of 2-MBT, where the interfacial oxide was comparatively thinner (~0.2 nm), only formed 1.2 – 1.5 nm thick 2-MBT layers.

Despite the thickness variations, the 2-MBT layer in the alkaline environment covered the entire surface with minimal defects, similar to that observed in the acidic environment, resulting in no thickness increase of the oxide islands on longer exposure time to the inhibitor-containing alkaline solution. Since the experiments in alkaline media were conducted in the absence of corrosive chloride ions, we do not know what effect the chloride ions would have on surfaces where the oxide film is stable and what role would the metal-organic complexes play on corrosion protection.

The mechanisms of 2-MBT adsorption in neutral chloride solution exhibit middling characteristics from that observed in acidic chloride and alkaline media. This is in part due to the presence of both thione and thiolate forms of the 2-MBT molecules in environments where the pH is between 4 and 9 [24]. Given that the pH of the environment of the present work was towards the lower side, between 5.2 to 5.5, the estimated thicknesses of the 2-MBT layers formed by each pre-treatment method are similar to those observed in the acidic environment conditions, as the thione form would be more prevalent. Since the thiolate form is also present in this pH environment, like in the alkaline environment, the bonding of the molecules to metallic copper by nitrogen atoms is rather compelling. The other factor, which seems to be the more consequential one, is the behaviour of copper in the different environments and its interaction with chloride ions. Due to the possible oxidation of copper at this pH, we did observe oxidation of the surface regions uncovered by defective 2-MBT

layer, especially during increased exposure time to the solution. The defects are most likely caused by the penetrating effect of chlorides in the organic barrier layer. The resulting oxidation of the surface leads to the growth of oxide islands which then enhances the formation of the metal-organic complexes, thus inducing an increase of the surface roughness revealed by ToF-SIMS depth profiling. Therefore, despite the similarities in bonding mechanisms of the 2-MBT molecules realized between the Cl-free alkaline and Cl-containing near neutral (NaCl) environments, there are features that are specific to the NaCl environment only and that we hope to have clarified in the present work.

Conclusion

The inhibition of corrosion initiation of copper by 2-MBT was investigated in a near neutral NaCl solution after the adsorption of the organic inhibitor. It is shown that 2-MBT adsorbs on the copper surface regardless of the surface state, altered using cathodic reduction pre-treatment methods of the native oxide layer. The 2-MBT molecules bond to the metallic substrate mostly by their sulphur atoms along with a very small fraction of nitrogen bonding with the metallic substrate. The interactions between the molecule and interfacial copper oxide occur most likely through the sulphur atoms of the molecule. However, the structure of the 2-MBT film and its protective properties highly depends on the surface state (interface) obtained after the pre-treatment methods used.

When the native oxide-covered surface is pre-treated with 2-MBT in the solution, a large coverage of the interfacial oxide still persists. The 2-MBT layer is relatively thin with Cu-2-MBT metal-organic complexes deposited on top, formed by an interaction between the Cu(I) ions (from Cu_2O) and the 2-MBT molecules. When pre-treated without 2-MBT in the solution, a wider coverage of the molecule adsorption is observed along with the formation of a thicker 2-MBT layer, even after just 2 minutes of exposure to 2-MBT, owing to lower amounts of interfacial oxide subsisting at the interface. A longer exposure time (1 hour) to 2-MBT after pre-treatment in its absence increases the thickness of the organic layer, but also results in a thickness increase of the interfacial oxide islands due to oxidation of the substrate at the defective regions of the 2-MBT layer. The formation of complexes is dependent on the quantity of interfacial oxides present, with a higher quantity of interfacial oxide resulting in an increased formation of the Cu-2-MBT metal-organic complexes.

Upon anodic polarization, the substrate pre-treated with 2-MBT shows reduced anodic activity compared to the substrate polarized in the reference NaCl solution. Surface analysis revealed an increase in the 2-MBT layer thickness after polarization and right before the initiation of corrosion, which is most likely due to the formation of further Cu-2-MBT complexes owing to the release of Cu(I) ions upon polarization. Despite this, no additional protection was offered to the substrate by the complexes. Pre-treatment in absence of 2-MBT followed by 2 minutes exposure to the inhibitor results in no anodic oxidation peak and a positive shift of the potential for corrosion initiation, indicative of better protective properties of the organic barrier layer formed. Longer exposure time to 2-MBT results in a higher positive shift of the potential for corrosion initiation. This further enhanced barrier properties of the inhibited interface results from both the higher coverage of the 2-MBT molecule on the surface and the thicker 2-MBT organic layer.

It is shown that the 2-MBT adsorption mechanisms on copper in a near neutral chloride environment is between that of the acidic and alkaline environment. This is mainly due to the dominant conformer of the molecule which depends on the pH of the environment, and the presence of chloride ions which compete with 2-MBT to adsorb on the surface. These factors are established as the defining conditions for the adsorption of 2-MBT on copper and subsequently the protection against corrosion in the neutral chloride environment.

Credit authorship contribution statement

Vishant Garg: Investigation, Formal analysis, Writing – original draft, review & editing.

Sandrine Zanna: Investigation, Validation, Writing – review & editing.

Antoine Seyeux: Investigation, Validation, Writing – review & editing.

Frédéric Wiame: Conceptualization, Validation, Writing – review & editing, Supervision.

Vincent Maurice: Conceptualization, Validation, Writing – review & editing, Supervision, Funding acquisition.

Philippe Marcus: Conceptualization, Writing – review & editing, Supervision, Funding acquisition, Project management.

Declaration of competing interest

The authors declare that they have no known competing financial interests or personal relationships that could have appeared to influence the work reported in this paper.

Acknowledgements

This project has received funding from the European Research Council (ERC) under the European Union's Horizon 2020 research and innovation program (ERC Advanced grant no. 741123).

Data availability

All data presented herein will be provided upon reasonable request.

References

[1] P. Marcus, V. Maurice, H.H. Strehblow, Localized corrosion (pitting): A model of passivity breakdown including the role of the oxide layer nanostructure, Corros Sci. 50 (2008) 2698–2704. https://doi.org/10.1016/j.corsci.2008.06.047.

[2] A. Fateh, M. Aliofkhazraei, A.R. Rezvanian, Review of corrosive environments for copper and its corrosion inhibitors, Arabian Journal of Chemistry. 13 (2020) 481–544. https://doi.org/10.1016/j.arabjc.2017.05.021.

[3] N. Takeno, Atlas of Eh-pH diagrams Intercomparison of thermodynamic databases, Geological Survey of Japan Open File Report. 419 (2005) 102.

[4] G. Kear, B.D. Barker, F.C. Walsh, Electrochemical corrosion of unalloyed copper in chloride media--a critical review, Corros Sci. 46 (2004) 109–135. https://doi.org/10.1016/S0010-938X(02)00257-3.

[5] A. Srivastava, R. Balasubramaniam, Microstructural characterization of copper corrosion in aqueous and soil environments, Mater Charact. 55 (2005) 127–135. https://doi.org/10.1016/j.matchar.2005.04.004.

[6] Y. Van Ingelgem, A. Hubin, J. Vereecken, Investigation of the first stages of the localized corrosion of pure copper combining EIS, FE-SEM and FE-AES, Electrochim Acta. 52 (2007) 7642–7650. https://doi.org/10.1016/j.electacta.2006.12.039.

[7] A. El Warraky, H.A. El Shayeb, E.M. Sherif, Pitting corrosion of copper in chloride solutions, Anti-Corrosion Methods and Materials. 51 (2004) 52–61. https://doi.org/10.1108/00035590410512735.

[8] G.S. Frankel, Pitting Corrosion of Metals: A Review of the Critical Factors, J Electrochem Soc. 145 (1998) 2186–2198. https://doi.org/10.1149/1.1838615.

[9] Lin L.F., Chao C.Y., Macdonald D.D., A Point Defect Model for Anodic Passive Films: II. Chemical Breakdown and Pit Initiation, J Electrochem Soc. 128 (1981). https://doi.org/10.1149/1.2127592.

[10] V. Maurice, P. Marcus, Current developments of nanoscale insight into corrosion protection by passive oxide films, Curr Opin Solid State Mater Sci. 22 (2018) 156–167. https://doi.org/10.1016/j.cossms.2018.05.004.

[11] W. Khalil, S. Haupt, H. -H Strehblow, The thinning of the passive layer of iron by halides, Materials and Corrosion. 36 (1985) 16–21. https://doi.org/10.1002/maco.19850360104.

[12] H. Parangusan, J. Bhadra, N. Al-Thani, A review of passivity breakdown on metal surfaces: influence of chloride- and sulfide-ion concentrations, temperature, and pH, Emergent Mater. 4 (2021) 1187–1203. https://doi.org/10.1007/s42247-021-00194-6.

[13] F. King, Corrosion of copper in alkaline chloride environments, Integrity Corrosion Consulting Ltd., Canada, & Swedish Nuclear Fuel and Waste Management Co., Sweden, 2002.

[14] M.G. Figueroa, R.C. Salvarezza, A.J. Arvia, The Influence of temperature on the pitting corrosion of copper, Electrochim Acta. 31 (1986) 665–669. https://doi.org/10.1016/0013-4686(86)87033-5.

[15] E. Touzé, C. Cougnon, Study of the air-formed oxide layer at the copper surface and its impact on the copper corrosion in an aggressive chloride medium, Electrochim Acta. 262 (2018) 206–213. https://doi.org/10.1016/j.electacta.2017.12.187.

[16] X. Wu, F. Wiame, V. Maurice, P. Marcus, 2-Mercaptobenzothiazole corrosion inhibitor deposited at ultra-low pressure on model copper surfaces, Corros Sci. 166 (2020) 108464. https://doi.org/10.1016/j.corsci.2020.108464.

[17] X. Wu, F. Wiame, V. Maurice, P. Marcus, Effects of water vapour on 2-mercaptobenzothiazole corrosion inhibitor films deposited on copper, Corros Sci. 189 (2021) 109565. https://doi.org/10.1016/j.corsci.2021.109565.

[18] X. Wu, F. Wiame, V. Maurice, P. Marcus, Moiré Structure of the 2-Mercaptobenzothiazole Corrosion Inhibitor Adsorbed on a (111)-Oriented Copper Surface, Journal of Physical Chemistry C. 124 (2020) 15995–16001. https://doi.org/10.1021/acs.jpcc.0c04083.

[19] V. Garg, S. Zanna, A. Seyeux, F. Wiame, V. Maurice, P. Marcus, Adsorption of 2-Mercaptobenzothiazole Organic Inhibitor and its Effects on Copper Anodic Oxidation in Alkaline Environment, J Electrochem Soc. 170 (2023) 071502. https://doi.org/10.1149/1945-7111/ace33b.

[20] V. Garg, S.B. Sharma, S. Zanna, A. Seyeux, F. Wiame, V. Maurice, P. Marcus, Enhanced corrosion inhibition of copper in acidic environment by cathodic control of interface

formation with 2-mercaptobenzothiazole, Electrochim Acta. 447 (2023) 142162. https://doi.org/10.1016/j.electacta.2023.142162.

[21] E. Vernack, S. Zanna, A. Seyeux, D. Costa, F. Chiter, P. Tingaut, P. Marcus, ToF-SIMS, XPS and DFT study of the adsorption of 2-mercaptobenzothiazole on copper in neutral aqueous solution and corrosion protection in chloride solution, Corros Sci. 210 (2023) 110854. https://doi.org/10.1016/j.corsci.2022.110854.

[22] R. Woods, G.A. Hope, K. Watling, A SERS spectroelectrochemical investigation of the interaction of 2-mercaptobenzothiazole with copper, silver and gold surfaces, J Appl Electrochem. 30 (2000) 1209–1222. https://doi.org/10.1023/A:1026561914338.

[23] D. Chadwick, T. Hashemi, Electron spectroscopy of corrosion inhibitors: Surface films formed by 2-mercaptobenzothiazole and 2-mercaptobenzimidazole on copper., Surf Sci. 89 (1979) 649–659. https://doi.org/10.1016/0039-6028(79)90646-0.

[24] M. Ohsawa, W. Suetaka, Spectro-electrochemical studies of the corrosion inhibition of copper by mercaptobenzothiazole, Corros Sci. 19 (1979) 709–722. https://doi.org/10.1016/S0010-938X(79)80142-0.

[25] M. Finšgar, D. Kek Merl, An electrochemical, long-term immersion, and XPS study of 2-mercaptobenzothiazole as a copper corrosion inhibitor in chloride solution, Corros Sci. 83 (2014) 164–175. https://doi.org/10.1016/j.corsci.2014.02.016.

[26] Y.S. Tan, M.P. Srinivasan, S.O. Pehkonen, S.Y.M. Chooi, Self-assembled organic thin films on electroplated copper for prevention of corrosion, Journal of Vacuum Science & Technology A: Vacuum, Surfaces, and Films. 22 (2004) 1917–1925. https://doi.org/10.1116/1.1763901.

[27] S.B. Sharma, V. Maurice, L.H. Klein, P. Marcus, Local Inhibition by 2-mercaptobenzothiazole of Early Stage Intergranular Corrosion of Copper, J Electrochem Soc. 167 (2020) 161504. https://doi.org/10.1149/1945-7111/abcc36.

[28] V. Brusic, M.A. Frisch, B.N. Eldridge, F.P. Novak, F.B. Kaufman, B.M. Rush, G.S. Frankel, Copper Corrosion With and Without Inhibitors, J Electrochem Soc. 138 (1991) 2253. https://doi.org/10.1149/1.2085957.

[29] A.C. Balaskas, M. Curioni, G.E. Thompson, Effectiveness of 2-mercaptobenzothiazole, 8-hydroxyquinoline and benzotriazole as corrosion inhibitors on AA 2024-T3 assessed by electrochemical methods, Surface and Interface Analysis. 47 (2015) 1029–1039. https://doi.org/10.1002/sia.5810.

[30] P. Visser, H. Terryn, J.M.C. Mol, On the importance of irreversibility of corrosion inhibitors for active coating protection of AA2024-T3, Corros Sci. 140 (2018) 272–285. https://doi.org/10.1016/j.corsci.2018.05.037.

[31] S.B. Sharma, V. Maurice, L.H. Klein, P. Marcus, Local Effects of Organic Inhibitor Molecules on Passivation of Grain Boundaries Studied In Situ on Copper, J Electrochem Soc. 168 (2021) 061501. https://doi.org/10.1149/1945-7111/ac0308.

[32] F. Chiter, D. Costa, V. Maurice, P. Marcus, DFT investigation of 2-mercaptobenzothiazole adsorption on model oxidized copper surfaces and relationship with corrosion inhibition, Appl Surf Sci. 537 (2021) 147802. https://doi.org/10.1016/j.apsusc.2020.147802.

[33] F. Chiter, D. Costa, V. Maurice, P. Marcus, Corrosion inhibition at emergent grain boundaries studied by DFT for 2-mercaptobenzothiazole on bi-crystalline copper, Npj Mater Degrad. 7 (2023) 5. https://doi.org/10.1038/s41529-022-00314-5.

[34] I.A. Arkhipushkin, Yu.E. Pronin, S.S. Vesely, L.P. Kazansky, Electrochemical and XPS study of 2-mercaptobenzothiazole nanolayers on zinc and copper surface, International Journal of Corrosion and Scale Inhibition. 3 (2014) 078–088. https://doi.org/10.17675/2305-6894-2014-3-2-078-088.

[35] M. Pourbaix, Atlas of Electrochemical Equilibria in-Aqueous Solutions, NACE, 1966.

[36] S. Mirhashemihaghighi, J. Światowska, V. Maurice, A. Seyeux, L.H. Klein, E. Härkönen, M. Ritala, P. Marcus, Electrochemical and Surface Analysis of the Corrosion Protection of Copper by Nanometer-Thick Alumina Coatings Prepared by Atomic Layer Deposition, J Electrochem Soc. 162 (2015) C377–C384. https://doi.org/10.1149/2.0081508jes.

[37] J.H. Scofield, Hartree-Slater Subshell Photoionization cross-sections at 1254 and 1487 eV, J Electron Spectros Relat Phenomena. 8 (1976) 129–137. https://doi.org/10.1016/0368-2048(76)80015-1.

[38] H. Shinotsuka, S. Tanuma, C.J. Powell, Calculations of electron inelastic mean free paths. XIII. Data for 14 organic compounds and water over the 50 eV to 200 keV range with the relativistic full Penn algorithm, Surface and Interface Analysis. 54 (2022) 534–560. https://doi.org/10.1002/sia.7064.

[39] F. Wiame, F.R. Jasnot, J. Światowska, A. Seyeux, F. Bertran, P. Le Fèvre, A. Taleb-Ibrahimi, V. Maurice, P. Marcus, Oxidation of α-brass: A photoelectron spectroscopy study, Surf Sci. 641 (2015) 51–59. https://doi.org/10.1016/j.susc.2015.05.013.

[40] A. Galtayries, J.P. Bonnelle, XPS and ISS studies on the interaction of H2S with polycrystalline Cu, Cu2O and CuO surfaces, Surface and Interface Analysis. 23 (1995) 171–179. https://doi.org/10.1002/sia.740230308.

[41] G. Deroubaix, P. Marcus, X-ray photoelectron spectroscopy analysis of copper and zinc oxides and sulphides, Surface and Interface Analysis. 18 (1992) 39–46. https://doi.org/10.1002/sia.740180107.

[42] J.F. Moulder, W.F. Stickle, P.E. Sobol, K.D. Bomben, J. Chastain, Handbook of X-ray Photoelectron Spectroscopy: A Reference Book of Standard Spectra for Identification and Interpretation of XPS Data, PerkinElmer Corporation, Eden Prairie, Minnesota, 1992.

[43] J.P. Chesick, J. Donohue, The molecular and crystal structure of 2-mercaptobenzothiazole, Acta Crystallogr B. 27 (1971) 1441–1444. https://doi.org/10.1107/s0567740871004102.

[44] J.W. Diggle, T.C. Downie, C.W. Goulding, Anodic Oxide Films On Aluminum, Chem Rev. 69 (1969) 365–405. https://doi.org/10.1021/cr60259a005.

[45] A.K. Rai, R. Singh, K.N. Singh, V.B. Singh, FTIR, Raman spectra and ab initio calculations of 2-mercaptobenzothiazole, Spectrochim Acta A Mol Biomol Spectrosc. 63 (2006) 483–490. https://doi.org/10.1016/j.saa.2005.05.034.

[46] B. Ellis, P.J.F. Griffiths, The ultra-violet spectra of some heterocyclic thioamides and hydrogen bonding, Spectrochimica Acta. 22 (1966) 2005–2032. https://doi.org/10.1016/0371-1951(66)80051-6.